# Molecular Basis for p38 Protein Kinase Inhibitor Specificity

**ARTICLE** *in* BIOCHEMISTRY · DECEMBER 1998

Impact Factor: 3.02 · DOI: 10.1021/bi981591x · Source: PubMed

# Molecular Basis for p38 Protein Kinase Inhibitor Specificity

JeanMarie Lisnock,[‡,§] Andy Tebben,[‡,§] Betsy Frantz,[∥] Edward A. O'Neill,[∥] Gist Croft,[∥] Stephen J. O'Keefe,[∥] Bing Li,[⊥] Candice Hacker,[⊥] Stephen de Laszlo,[⊥] Anthony Smith,[⊥] Brian Libby,[⊥] Nigel Liverton,[⊥] Jeffrey Hermes,[‡] and Philip LoGrasso*[,‡]

*Departments of Molecular Design and Diversity, Medicinal Chemistry, and Immunology and Inflammation, Merck Research Laboratories, P.O. Box 2000, Building R50A-300, Rahway, New Jersey 07065, and Sumneytown Pike, P.O. Box 4, West Point, Pennsylvania 19486*

*Received July 6, 1998; Revised Manuscript Received September 17, 1998*

ABSTRACT: p38 is a member of the mitogen-activated protein (MAP) kinase family and is a critical enzyme in the proinflammatory cytokine pathway. Other MAP kinase group members that share both structural and functional homology to p38 include the c-Jun $NH_2$-terminal kinases (JNKs or SAPKs) and the extracellular-regulated protein kinases (ERKs). In this study, we determined the molecular basis for p38α inhibitor specificity exhibited by five compounds in the diarylimidazole, triarylimidazole, and triarylpyrrole classes of protein kinase inhibitors. These compounds are significantly more potent inhibitors of p38 compared to the JNKs and ERKs. Three active site ATP-binding domain residues in p38, T106, M109, and A157, selected based on primary sequence alignment, molecular modeling, and X-ray crystal structure data, were mutated to assess their role in inhibitor binding and enzymatic catalysis. All mutants, with the exception of T106M, had kinase activity within 3-fold of wild-type p38. Mutation of T106 to glutamine, the residue present at the corresponding position in ERK-2, or methionine, the corresponding residue in p38γ, p38δ, and the JNKs, rendered all five inhibitors ineffective. The diarylimidazoles had approximately a 6-fold decrease in potency toward M109A p38. For the mutant A157V, all diarylimidazoles and triarylimidazoles tested were 5−10-fold more potent compared with wild-type p38. In contrast, two triarylpyrroles were 15−40-fold less potent versus A157V p38. These results showed that the molecular basis for the specificity of the p38 inhibitors was attributed largely to threonine 106 in p38 and that methionine 109 contributes to increased binding affinity for imidazole based inhibitors.

The serine/threonine (Ser/Thr) kinases and tyrosine kinases are enzymes that phosphorylate either serine or threonine residues or tyrosine residues on a variety of proteins, many of which are involved in signal transduction pathways associated with a variety of cellular processes (*1, 2*). These kinases have been implicated in a number of signaling pathways contributing to disease states, including cancer (*3, 4*), psoriasis (*5*), atherosclerosis (*6*), and chronic inflammatory diseases such as rheumatoid arthritis and inflammatory bowel disease (*7, 8*). Thus, inhibition of protein kinase activity and concomitant interruption of signal transduction is a potential route for therapeutic intervention. A number of reports describe various classes of inhibitors for tyrosine kinases (*9*−*11*), and recently, a series of reports have described a class of pyridinyl imidazoles that are selective inhibitors for p38 MAP[1] kinase (*12*−*15*).

p38 is a MAP kinase that was first shown to be phosphorylated and activated in response to lipopolysaccharide (LPS or endotoxin) (*16*) and has subsequently been shown to be activated by other environmental stimuli such as TNF-α, IL-1β, and hyperosmolality (*17, 18*). Activation of p38 follows a distinct protein kinase cascade in which the upstream activator of p38 is classified as a MAP kinase kinase (MKK). MKK6, MKK4, MKK3, and MKK3-b are dual specificity kinases that phosphorylate p38 on both Thr and Tyr in the activation loop and have been shown in vivo and in vitro to be direct upstream activators of p38 (*18*−*21*). Several downstream substrates for p38 have been suggested including MAPKAP-2, MAPKAP-3, and ATF-2 (*14, 18, 22, 23*), and the kinetic mechanism for p38 has been shown to be ordered sequential with protein substrate (GST-ATF2) binding before ATP (*24*).

The crystal structure of unphosphorylated p38 has been described (*25, 26*) as well as crystal structures of unphosphorylated p38 complexed with two different pyridinyl imidazoles (*27, 28*). Comparison of the primary amino acid sequences of p38 with extracellular-regulated protein kinase (ERK-2) reveals approximately 40% homology, and com-

* To whom correspondence should be addressed. Phone: (732) 594-1271. E-mail: lograsso@merck.com.

‡ Department of Molecular Design and Diversity.

§ These authors contributed equally to the work.

∥ Department of Immunology and Inflammation.

⊥ Department of Medicinal Chemistry.

[1] Abbreviations: ATF-2, activating transcription factor 2; cAPK, cyclic AMP-dependent protein kinase; DTT, dithiothreitol; EDTA, ethylenediaminetetraacetic acid; ERK-2, extracellular-regulated protein kinase 2; GST, glutathione *S*-transferase; HEPES, *N*-(2-hydroxyethyl)-piperazine-*N*′-2-ethanesulfonic acid; IL-1, interleukin-1; IPTG, isopropyl thio-β-D-galactoside; JNKs, c-jun $NH_2$-terminal kinases; LPS, lipopolysaccharide; MAP, mitogen-activated protein kinase; MAPKAP kinase, mitogen-activated protein kinase-activated protein kinase; MBP, myelin basic protein; MKK, MAP kinase kinase; PAGE, polyacrylamide gel electrophoresis; SAPKs, stress-activated protein kinase; TNF, tumor necrosis factor.

10.1021/bi981591x CCC: $15.00 
Published on Web 11/01/1998

parison of the structure of the C-terminal and N-terminal lobes showed a rms deviation of 0.8 and 1.2 Å, respectively (*26*). In addition to the ERKs, p38 shares sequence similarity and conserved structural domains with the Jun N-terminal kinases (JNKs) and to a lesser extent with cyclic AMP-dependent kinase (cAPK), the historical paradigm for Ser/Thr kinases. With such structural similarity between the Ser/Thr kinases, and surprisingly strong similarity between the Ser/Thr kinases and the Tyr kinases [comparing C-terminal and N-terminal lobes of cAPK and lck shows C-terminal rms deviation = 1.2 Å and N-terminal = 1.18 Å (*29*)], it is of interest to determine how small molecules might be specific inhibitors of a particular kinase. Most inhibitors of kinases have been shown to bind in the ATP pocket (*27, 28, 30*−*32*) and are competitive inhibitors with respect to ATP (*9, 24, 33*−*35*).

In our work, we employed site-directed mutagenesis to determine what residues in p38 were essential for inhibitor binding. To do this, three p38 ATP-binding domain residues were mutated based on primary sequence alignment, molecular modeling, and X-ray crystal structure data for p38, and the $IC_{50}$ values for five inhibitors of differing structure were determined. The major findings of this study include threonine 106 is a major determinant for p38 inhibitor specificity; methionine 109 contributes to increased binding affinity for the diarylimidazoles, and the residue at position 157 influences binding affinity of all compounds by altering the position of the M109 side chain. Furthermore, our data demonstrate that, despite the structural similarity among all of the protein kinases, selective, subnanomolar inhibitors that bind in the ATP-pocket of p38 are possible.

## MATERIALS AND METHODS

*Mutagenesis.* Wild-type human p38α was subcloned into a pET30(a)+ (Novagen) vector altered to contain a modified N-terminal FLAG (Kodak) peptide sequence (MDYKDDDDHMHG) and a 5′ *Bam*HI cloning site. The A157V and M109A p38 mutants were generated utilizing the QuikChange Site-Directed Mutagenesis method (Stratagene) following the manufacturer's protocol. Oligonucleotides A and B or C and D (Gibco BRL) were used to create the mutations at A157V and M109A, respectively:

(A) 5′-CCTAGTAATCTAGTTGTGAATGAA-GACTGTG-3′

(B) 5′-ACAGTCTTCATTCACAACTAGAT-TACTAGG-3

(C) 5′-GTGACCCATCTCGCTGGGGCAGATCTG-3′

(D) 5′-CAGATCTGCCCCAGCGAGATGGGTCAC-3′

Mutations were confirmed by DNA sequencing of the entire p38 sequence (1.2 kb) utilizing the Perkin-Elmer ABI PRISM DNA sequencing method.

*Cassette Mutagenesis.* Unique restriction sites were introduced by QuikChange Mutagenesis (Stratagene) into the pET30(a)+ FLAG p38 vector so that a 53 base pair cassette (*36*) region spanning nucleotides 663−716 (*12*) could be inserted for mutational analysis. An *Aat*II restriction site was introduced at the 5′ end of the cassette between nucleotides 663 and 668 (amino acids 101−102), and an *Afl*II site was introduced at the 3′ end of the cassette between nucleotides 711 and 716 (amino acids 117−118). These sites were introduced individually using the following oligonucleotides:

*Aat*II

(E) 5′-GAGGAATTCAATGACGTCTATCT-GGTGACC-3′

(F) 5′-GGTCACCAGATAGACGTCATTGA-ATTCCTC-3′

*Afl*II

(G) 5′-CTGAACAACATTCTTAAGTGTCAGA-AGCTTAC-3′

(H) 5′-GTAAGCTTGTGACACTTAAGAATGT-TGTTCAG-3′

The presence of both sites was confirmed by restriction digest and DNA sequencing.

The desired cassette mutants were created by digesting 5 μg of the above p38 cassette vector with *Afl*II (NEB) at 1.25 units/mL for 1 h at 37 °C followed by restriction with *Aat*II (NEB) at 2 units/ml for 1 h at 37 °C. The vector fragment generated was isolated by 1% agarose gel electrophoresis, and purified by Qiaex II gel extraction (Qiagen). Complementary oligonucleotides (Gibco BRL) were designed for ligation within the cassette vector and contained the desired p38 mutations T106Q and T106M. The sequence for the two T106 mutants is given below:

T106Q

(I) 5′-CTATCTGGTGCAGCATCTCATGGGGGCA-GATCTGAACAACATTG-3′

(J) 5′-TTAACAATGTTGTTCAGATCTGCCCCCA-TGAGATGCTGCACCAGATAGACGT-3′

T106M

(K) 5′-CTATCTGGTGATGCATCTCATGGGGGC-AGATCTGAACAACATTG-3′

(L) 5′-TTAACAATGTTGTTCAGATCTGCCCCCA-TGAGATGCATCACCAGATAGACGT-3′

Complementary oligonucleotides were annealed to create double-stranded inserts by heating to 90 °C in 20 μL of ligase buffer (NEB), 150 mM NaCl (Digene), 10 μM primer I, and 10 μM primer J (or 10 μM primer K and 10 μM primer L) followed by slow cooling to 25 °C. The double-stranded inserts were ligated to the *Afl*II/*Aat*II restricted vector using 1 μM double stranded insert and 0.1 μg of *Afl*II/*Aat*II-restricted pET30a(+) p38. The ligation reaction was performed at 22 °C for 2 h using high concentration ligase (NEB) at 100 units/mL. Following ligation, 25 μL of 10 mM Tris-HCl, pH 8.0, and 1 mM EDTA was added to the 20 μL ligation reactions and the mixture was reannealed by heating to 90 °C and cooling to 22 °C to avoid potential inserts of linker concatomers (*36*). Two microliters of the ligation reaction was transformed into 20 μL of XL-1 Blue competent cells (Stratagene) and plated on LB + 1.5% agar, pH 7.3 (Digene), containing 50 μg/mL Kanamycin (Sigma).

pET30(a)+ FLAG p38 T106Q and pET30(a)+ FLAG p38 T106M were isolated, and restriction analysis and DNA sequencing confirmed the desired mutations.

*Expression of p38 Mutants.* All p38 mutants were expressed in *Escherichia coli* strain BL21 (DE3) pLysS (Novagen) under the following conditions: 500 mL of LB medium, pH 7.3 (Digene), containing 50 $\mu$g/mL Kanamycin (Sigma) and 30 $\mu$g/mL chloramphenicol (Sigma) was inoculated with 10 mL of a saturated culture of BL21 (DE3) pLysS harboring the pET30a(+) Flag p38 A157V, M109A, T106Q, or T106M plasmids and grown with agitation at 225 rpm at 37 °C until the culture reached an $OD_{600} = 0.8$. The culture was centrifuged at 2830*g* for 10 min at 4 °C. The pellet was resuspended in minimal media M9 salts (Gibco), 10% cas amino acids (Sigma), 100 $\mu$M $CaCl_2$ (Sigma), 2 mM $MgSO_4$ (Sigma), 50 $\mu$g/mL Kanamycin (Sigma), and 30 $\mu$g/mL chloramphenicol (Sigma) and induced with isopropylthio-$\beta$-D-galactoside (IPTG) (Gibco) at a final concentration of 0.5 mM. The cultures were grown at 18 °C for 18 h and harvested by centrifugation at 2380*g* for 10 min. The pellets were frozen at −70 °C.

*Purification of p38 Mutants.* Frozen *E. coli* cell pellets from 250 mL of culture were resuspended in 12 mL of buffer containing 10 mM Tris-HCl, pH 7.4 (Digene), 150 mM NaCl (Digene), 10 mM DTT (Sigma), 10% glycerol (Sigma), 1 $\mu$g/mL each of bestatin, leupeptin, aprotinin, pepstatin A (Sigma), and 2.5 $\mu$g/mL DNAse I (Sigma) and refrozen. The pellet was rethawed and gently mixed at 4 °C for 45 min until the solution was no longer viscous. The suspension was centrifuged at 126086*g* for 1 h at 4 °C and the supernatant was used for subsequent purification. A 5 mL Anti-FLAG M2 (Kodak) antibody affinity column was equilibrated with 30 mL of column buffer containing: 10 mM Tris-HCl, pH 7.4 (Digene), 150 mM NaCl (Digene), 10 mM DTT (Sigma), and 10% glycerol (Sigma). For each mutant expressed, appropriate supernatant volumes were applied to the resin such that the binding capacity (2 mg/mL) of the resin was not exceeded. The column was washed with 5 bed volumes of column buffer containing 1 $\mu$g/mL each of bestatin, leupeptin, aprotinin, and pepstatin A (Sigma). p38 was eluted in 1 mL fractions at room temperature using warmed (42 °C) column buffer containing FLAG peptide at 500 $\mu$g/mL. Coomassie Brilliant Blue R-250 (Sigma) staining of SDS−PAGE 12% Tris-glycine gels (Novex) revealed greater than 95% homogeneity of all p38 proteins. Protein concentration was determined by Bradford assay (Bio-Rad).

*Cloning, Expression, and Purification of MKK6-EE Constitutively Active Mutant.* cDNA encoding MKK6 (*20*) was generated from human skeletal muscle RNA (Clontech) using the GeneAmp protocol (Perkin-Elmer). The cDNA was modified to encode an N-terminal FLAG epitope (Kodak) and was subcloned into plasmid pUC18. Serine 207 and threonine 211 were mutated to glutamates by PCR site-directed mutagenesis: the codon for Ser 207 (nucleotides 619−621, TCT) was substituted with the codon for Glu 207 (GAG); the first two bases of the codon for Thr 211-(nucleotides 631−633, ACA) were substituted to yield a degenerate codon for Glu 211 (GAA). A novel *Cla*I restriction site was incorporated into the cDNA by mutagenesis of nucleotide 636T to C. This mutation did not change the identity of amino acid 212. Plasmid DNA was purified using the Qiagen Plasmid Midi Kit (Qiagen), sequenced with an ABI Prism DNA Sequencer and fluorescent sequencing reagents (Perkin-Elmer) and analyzed using Sequencher 3.0 (Gene Codes). The FLAG-MKK6EE cDNA was subcloned into the pRMHaS2neo plasmid [an insertion of pS2-neo [derived from pUChsneo (*37*)] into pRMHa-3 [derived from pRmHA-1 (*38*)]] under transcriptional control of a copper-inducible metallothionine promoter. The new plasmid (pRMHaS2neo-MKK6EE) was transfected into *Drosophila* Schneider S2 cells by calcium phosphate precipitation and enriched under G418 selection for 1 month following protocols from Gibco. FLAG-MKK6EE was expressed in and purified from the transfected cells (S2-FLAGMKK6EE) by the techniques described for the expression and purification of FLAG-p38 (*24*).

*Activation of p38 Mutants.* p38 mutants were activated in vitro by MKK-6 EE in 50 $\mu$L of a buffer containing 25 mM HEPES (Sigma), pH 7.4, 10 mM $MgCl_2$ (Sigma), 2 mM DTT (Sigma), 20 mM $\beta$-glycerophosphate (Sigma), 0.1 mM $Na_3VO_4$, 1 mM ATP (Sigma), 1 $\mu$M p38 mutant, and 10 nM MKK-6EE. Reactions were incubated at 30 °C for 2 h. The phosphorylated mutants were diluted to appropriate concentration and used as active p38 enzyme in either the steady-state kinetics or enzyme inhibition studies. Bis-phosphorylation of mutants was confirmed by mass spectrometry and western blotting utilizing a rabbit anti-human polyclonal antibody specific for bis-phosphorylated p38 (New England Biolabs).

*Steady-State Kinetics.* Initial velocity studies utilized to determine the steady-state constants for ATP and GST-ATF2 were carried out in 100 $\mu$L volumes containing the final concentrations of the following: 25 mM HEPES (Sigma) (pH 7.4); 10 mM $MgCl_2$ (Sigma); 2 mM DTT (Sigma); 20 mM $\beta$-glycerophosphate (Sigma); 0.1 mM $Na_3VO_4$ (Sigma); 4 $\mu$Ci [$\gamma$-$^{33}$P]ATP (2000 Ci/mmol; 1 Ci = 37 GBq) (Amersham); 2.5−250 $\mu$M ATP (Pharmacia); and 0.48−11.6 $\mu$M GST-ATF2. The reactions were initiated with the addition of 5 nM p38 (final concentration) and incubated for 60 min at 30 °C for all mutants except T106M which was incubated for 20 min. Under these conditions, less than 10% of substrate was converted to product. The reaction was shown to be linear over a time course up to 3 h for all mutants except T106M, which was linear for 30 min. Reactions were stopped with 100 $\mu$L of 100 mM EDTA/15 mM sodium pyrophosphate. Immobilon-P 96-well plates (Millipore MAIPNOB 10) were pretreated with 100 $\mu$L of methanol, followed by 100 $\mu$L of 15 mM sodium pyrophosphate. Fifty microliters of the stopped reaction was spotted in triplicate on the immobilon-P 96-well plate. The samples were vacuum-filtered and washed three times each with 100 $\mu$L of 75 mM $H_3PO_4$ to remove unicorporated [$\gamma$-$^{33}$P]ATP. After the third $H_3PO_4$ wash and a final filtration step to remove $H_3PO_4$, 50 $\mu$L of Microscint-20 (Packard) was added to each well and samples were analyzed on a Packard Topcount liquid scintillation counter. Data for T106M and wild-type are from the average of two experiments each filtered in triplicate. Data for T106Q, M109A, and A157V are from a single experiment filtered in triplicate. The initial velocities as a function of both GST-ATF2 and ATP were fitted to equations for ternary-complex (sequential) mechanism (*39*). Kinetic constants were determined from nonlinear least-squares analysis (*39*).

```
Codon      101                  106                                          117 118

WT 5′-AAT GAT GTG TAT CTG GTG ACC CAT CTC ATG GGG GCA GAT CTG AAC AAC ATT GTG AAA TGT CAG-3′

CS 5′-AAT GAC GTC TAT CTG GTG ACC CAT CTC ATG GGG GCA GAT CTG AAC AAC ATT CTT AAG TGT CAG-3′

MT 5′-AAT GAC GTC TAT CTG GTG NNN CAT CTC ATG GGG GCA GAT CTG AAC AAC ATT GTT AAG TGT CAG-3′

WT           D   V                T                                          V   K

CS           D   V                T                                          L   K

MT           D   V              (Q,M)                                        V   K
```

FIGURE 1: Cassette mutagenesis strategy. Line 1: The amino acid number for wild-type p38. Line 2: The coding DNA strand for wild-type p38(WT). Line 3: DNA sequence for the introduction of unique restiction sites (underlined) for cassette mutagenesis (CS). 5′ restriction site: *Aat*II; GACGTC. 3′ restriction site: *Afl*II; CTTAAG. Line 4: DNA sequence for mutagenic p38. NNN (bold) represents the codon for any amino acid. Line 5: amino acid sequence for wild-type p38 at selected codons. Line 6: amino acid sequence for cassette p38 at selected codons. Line 7: Amino acid sequence for mutant p38 at selected codons. In our experiments, either Q or M was inserted at codon 106.

| p38α aa # | 35 | 38 | 51 | 53 | 75 | 84 | 86 | 104 | 106 | 107 | 108 | 109 | 155 | 157 | 168 |
|---|---|---|---|---|---|---|---|---|---|---|---|---|---|---|---|
| p38α | Y | V | A | K | L | I | L | L | T | H | L | M | N | A | D |
| p38β | Y | V | A | K | L | I | L | L | T | **T** | L | M | N | A | D |
| p38γ | Y | V | A | K | L | I | L | L | **M** | **P** | **F** | M | N | A | D |
| p38δ | Y | V | A | K | L | I | L | L | **M** | **P** | **F** | M | N | A | D |
| JNK2β | Q | V | A | K | L | I | L | L | **M** | **E** | L | M | N | **V** | D |
| JNK2α | Q | V | A | K | L | I | L | L | **M** | **E** | L | M | N | **V** | D |
| ERK-2 | Y | V | A | K | L | I | **I** | **I** | **Q** | **D** | L | M | N | **L** | D |
| cAPK | **F** | V | A | K | L | **V** | L | **M** | **M** | **E** | **Y** | **V** | N | **L** | D |

FIGURE 2: Amino acid comparison between residues in p38α and homologous protein Ser/Thr kinases. Bold residues represent amino acids different from those in p38α. With the exception of histidine 107 and alanine 157 these residues were shown by molecular modeling to have at least one side-chain atom within 4 Å of any atom in L-786134.

*Enzyme Inhibition.* Enzyme inhibition studies were performed at 30 °C under the buffer conditions described above. GST-ATF2 concentration was fixed at 2 $\mu$M, and ATP concentration was fixed at 5 $\mu$M. Reaction times ranged from 1 h for SB203580 (Cal Biochem) (5 nM), L-167307 (5 nM), L-167782 (5 nM), and L-799543 (5 nM) to 18 h for L-786134 (50 pM). For T106M, the reaction time was 20 min for all compounds. Enzyme concentrations used for the various inhibitors are shown in brackets next to the inhibitor. $IC_{50}$ values were determined by fitting the data to the equation for a four parameter logistic (*39*). The errors shown are standard errors. Data are from the average of at least two experiments filtered in triplicate. Synthesis of L-167307 and L-167782 has been reported (*40*). L-786134 and L-799543 were sythesized with analogous chemistry to compounds which will be described [Liverton et al. (1998) *J. Med. Chem.* (submitted for publication)].

*Molecular Modeling.* p38 was modeled based on the apo p38 structure (*25*). The conformations of the Thr 106 and Met 109 side chains were modeled based on their positions in the VK-19911/p38 complex (*28*) and the water associated with Thr 106 was removed. The modified side-chain conformations were then minimized using the CHARMm[3] force field as implemented in Quanta97 (Molecular Simulations Inc.). All of the minimizations were carried out using the Adopted-Basis Newton Rapson minimization method to an rms force of 0.001. The inhibitors were docked into this model using the crystallographic conformation of VK-19911 and its position in the ATP-binding site as a guide. In addition to the contacts from the protein, it has been suggested that there are water molecules associated with VK-19911 (*28*). The initial docking of L-786134 indicated that a water could form a hydrogen-bonding network bridging the N3 nitrogen of the inhibitor imidazole, Lys 53, and Asp 168. A water was placed in the model at a position amenable to these interactions and was included in subsequent modeling. During minimization, the inhibitor and above-mentioned water were allowed to move freely and a harmonic force of 10 was placed on the side chains of any residue within 5 Å of the inhibitor. Initially, the protein backbone was frozen, but in the process of modeling L-786134, it appeared that a change in the backbone conformation of Asp 168 would be necessary to accommodate the piperidyl group of this inhibitor. Since residues 170−174 were unresolved in the apo crystal structure and high thermal factors were observed on Phe 169 and Asp 168, it seemed reasonable to allow some movement of the backbone of Asp 168 and Phe 169. The backbone of these two residues was restrained with a harmonic force of 10.

## RESULTS

*Preparation of p38 Mutants.* To investigate residues in the ATP-binding domain of p38 that may affect inhibitor binding and specificity, we employed a site-specific and cassette mutagenesis approach to probe this region. Cassette mutagenesis (*36*) allowed us to easily introduce point mutations in a region that spanned amino acids 101−118 (Figure 1). Unique restriction sites were introduced on the 5′ end beginning at nucleotides (*12*) 663−668 (amino acids 101−102) and on the 3′ end at nucleotides 711−716 (amino acids 117−118) (Figure 1). Using this method, we mutated Thr 106 to glutamine (the corresponding residue in ERK-2) and methionine (the corresponding residue in p38$\gamma$, p38$\delta$, the JNKs, and cAPK) (Figure 2). Other residues selected for site-specific mutagenesis were Met 109 and Ala 157. Comparison of these residues with corresponding sites on other kinases is shown in Figure 2.

Table 1: Steady-State Rate Constants for the Phosphorylation of GST-ATF2 Catalyzed by Wild-Type and Mutant p38 MAP Kinase

| p38 enzymes | $K_{m(GST-ATF2)}$ ($\mu$M) | $K_{m(ATP)}$ ($\mu$M) | $k_{cat}$ ($min^{-1}$) | $k_{cat}/K_{m(ATP)}$ ($\mu M^{-1}$ $min^{-1}$) |
|---|---|---|---|---|
| wild-type[a] | $6.2 \pm 0.6$ | $23 \pm 2$ | $4.8 \pm 0.2$ | $0.2 \pm 0.02$ |
| A157V | $3.8 \pm 1.3$ | $25 \pm 11$ | $10.6 \pm 1.3$ | $0.4 \pm 0.2$ |
| M109A | $2.9 \pm 0.3$ | $30 \pm 3$ | $14.7 \pm 0.6$ | $0.5 \pm 0.05$ |
| T106Q | $7.8 \pm 3.9$ | $397 \pm 175$ | $42 \pm 12$ | $0.1 \pm 0.05$ |
| T106M | $3.1 \pm 0.5$ | $15 \pm 3.4$ | $20 \pm 1.5$ | $1.3 \pm 0.4$ |

[a] From ref *24*. The kinetic parameters were calculated from the equation for a ternary complex (*39*). The errors shown are standard errors. Data for T106M and wild-type are from the average of two experiments each filtered in triplicate. Data for T106Q, M109A, and A157V are from a single experiment filtered in triplicate.

*Steady-State Kinetic Parameters.* The steady-state rate constants for the phosphorylation of GST-ATF2 catalyzed by wild-type and four mutants of p38 MAP kinase are presented in Table 1. Two-substrate profile analysis revealed that the $K_m$ of GST-ATF2 for all four p38 mutants was within 2-fold of wild-type p38 (Table 1). $K_m$ for ATP was unchanged for all mutants with the exception of T106Q which had $K_m$ for ATP approximately 17-fold greater than wild-type p38 (Table 1). Values of $k_{cat}$ differed 2−4-fold from wild-type p38 for the mutants A157V, M109A, and T106M. T106Q had $k_{cat}$ 9-fold greater than wild-type (Table 1). Finally, A157V, M109A, and T106Q had $k_{cat}/K_m$(ATP) within 2−3-fold of wild-type p38. Only T106M showed a greater than 5-fold increase of $k_{cat}/K_m$(ATP) from wild-type p38 (Table 1).

*Inhibitor Structure and Binding.* The structure of one triarylimidazole, two triarylpyrroles, and two diarylimidazoles utilized to assess how mutations at amino acids 106, 109, and 157 in p38 affected inhibitor binding are shown in Figure 3. SB203580 (Figure 3A) has been shown kinetically to be a competitive inhibitor with ATP [$K_i = 21$ nM (*34*); $K_i = 34$ nM (*24*)] and by X-ray crystallography to bind in the ATP pocket (*27*). L-167307 (Figure 3A) differs from SB203580 in that the central imidazole is replaced by a pyrrole in L-167307. Main features of L-786134, an example of the diarylimidazoles (Figure 3B), are the 4-trifluoromethylphenyl ring, the 5-pyridinyl and the 2-(4-piperidinyl) rings on the central imidazole.

A stereoview for the minimized model of L-786134 is presented in Figure 4A, and p38 residues contacting the inhibitor are shown in Figure 2. The pyridinyl ring at the 5-position of imidazole forms a hydrogen bond with the backbone amide proton of Met 109. This was also observed in the p38/VK-19911 complex (*28*). In addition, the pyridinyl ring forms stabilizing van der Waals contacts with the side chain of Met 109. The 4-trifluoromethylphenyl group on imidazole occupies a hydrophobic pocket close to the ATP-binding site, but not utilized by ATP (*26*−*28*). This hydrophobic pocket is partially formed by the side chain of Thr 106, which packs against the *m*-trifluorophenyl ring of L-786134. The piperidyl moiety on the 2-position of the imidazole forms a salt bridge with the carboxy group of Asp 168. The N3 nitrogen of the imidazole ring forms a hydrogen bond with an active-site water molecule. The position of this water is further stabilized by a hydrogen-bonding network involving the imidazole nitrogen, the side-chain nitrogen of Lys 53, and a side-chain oxygen of Asp 168.

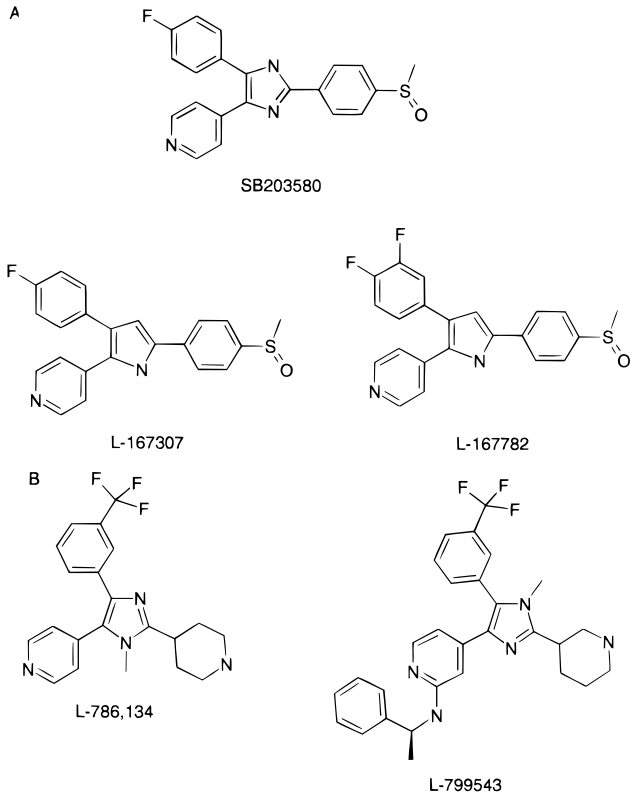


FIGURE 3: (A) Structure of one triaryimidazole and two triarylpyrroles. (B) Structure of two diarylimidazoles

Modeling of L-167307 (Figure 4B) revealed that many of the contacts observed in the L-786134 model were retained. The *p*-fluorophenyl ring fills the same pocket and forms similar hydrophobic contacts as the *m*-trifluoromethylphenyl ring of L-786134. The hydrogen bond from the pyridinyl ring to the backbone amide of Met 109 is also preserved. However, attempts at minimization of this inhibitor with a bridging water molecule similar to that in the L-786134 model did not result in the formation of a stable hydrogen-bonding network. The lack of this hydrogen bond combined with the loss of the salt bridge to the substituent in the 2-position resulted in the displacement of L-167307 relative to the position of L-786134 (Figure 4B). This displacement resulted in unfavorable contacts between the inhibitor and the extended side chain of Met 109. These contacts were removed upon minimization of a structure starting with the more folded conformation of the Met 109 side chain taken from the apo structure.

*Effects of Mutations on Inhibitor Binding.* The $IC_{50}$ values for five p38 inhibitors were measured against wild-type p38 and four ATP-binding domain mutants (Table 2). The most striking observation was that mutation of Thr 106 to Gln or Met rendered all compounds inactive versus these mutants (Table 2). For example, L-786134 has $IC_{50} = 7$ nM versus wild-type p38 but no inhibition of T106Q or T106M at concentrations at least 400-fold greater (3000 nM). Two other observations were that (1) mutation of Met 109 to Ala caused all the inhibitors to be less potent compared to wild-type p38 and (2) mutation of Ala 157 to Val caused the diarylimidazoles and the triarylimidazoles (Figure 3 panels B and A, respectively) to be more potent compared to wild-type p38, but the triarylpyrroles (Figure 3A) less potent compared to wild-type p38 (Table 2).

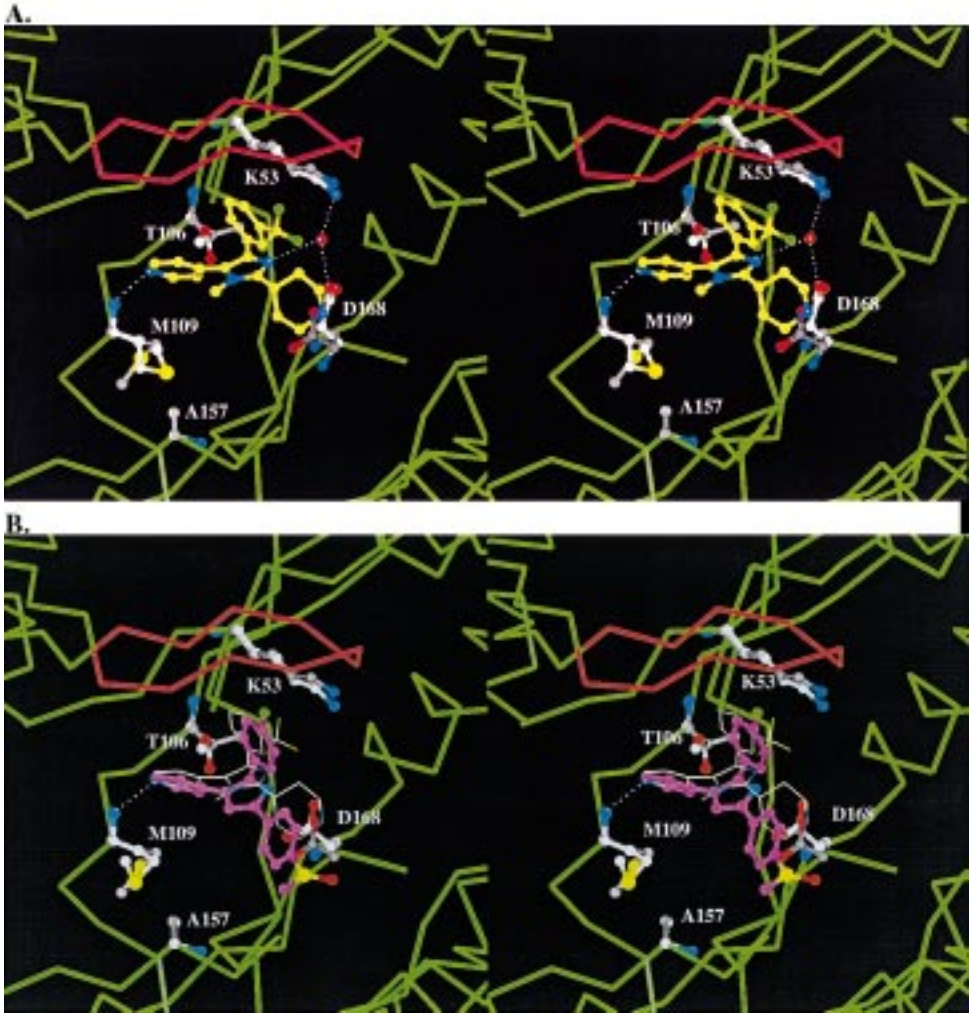


FIGURE 4: (A) Stereoview of L-786134 docked and minimized in the ATP-binding site of p38. Residues 106, 109, and 157 (balls) were mutated in this study. Hydrogen bonds are denoted with dotted lines and the active-site water molecule is shown in red. The residues from the minimized structure are colored white and the position of the residues from the apo structure (*25*) are indicated in gray. The α-carbon backbone is traced in green pipes and the glycine-rich flap is highlighted in red. (B) Stereoview for the comparison of the minimized structures for L-167307 (balls) and L-786134 (yellow wires). The p38 structure is colored as in Figure 4A.

Table 2: $IC_{50}$ (nM) for p38 Inhibitors versus ATP Active-Site Domain Mutants[a]

| compd | WT | A157V | M109A | T106Q | T106M |
|---|---|---|---|---|---|
| SB203580 | 30 ± 1.5 | 6 ± 0.5 | 120 ± 14 | NI[b] | NI |
| L-167307 | 4 ± 0.3 | 58 ± 8 | 7.5 ± 1.5 | NI | NI |
| L-167782 | 12 ± 3 | 450 ± 122 | 37 ± 8 | NI | NI |
| L-799543 | 94 ± 10 | 13 ± 2 | 712 ± 105 | NI | NI |
| L-786134 | 7 ± 0.2 | <0.5 | 46 ± 9 | NI | NI |

[a] $IC_{50}$ values were determined by fitting the data to the equation for a four parameter logistic (*39*). The errors shown are standard errors. Data are from the average of at least two experiments filtered in triplicate. [b] NI = no inhibition.

## DISCUSSION

Our study was designed to describe at the molecular level which ATP-binding domain residues of p38 contribute to selective inhibition by a series of diarylimidazoles, triarylimidazoles, and triarylpyrroles. To do this, we employed a site-directed mutagenesis approach that focused on amino acids 106, 109, and 157 in p38. Understanding the molecular basis for p38 inhibitor specificity is of great interest given the fact that many kinases share close structural similarity (*26*, *29*) and most kinase inhibitors have been shown to be competitive with ATP (*9*, *24*, *33*−*35*).

In the past several years, a number of potent, selective inhibitors of a variety of protein kinases (*9*, *33*, *41*, *42*) and p38 in particular (*14*, *15*) have been reported. Four crystal structures of p38 have been reported: two for the unphosphorylated, uncomplexed form (*25*, *26*) and two for the unphosphorylated-inhibitor bound form (*27*, *28*). Information from these structures has helped elucidate the key features of the p38 ATP-binding site and begun to define those residues important for inhibitor binding. Wilson et al. (*28*) defined 14 residues in p38 (Val 38; Ala 51; Lys 53; Leu 75; Ile 84; Leu 86; Leu 104; Val 105; Thr 106; His 107; Leu 108; Met 109; Leu 167; and Asp 168) that have at least one atom within 4 Å of any atom in VK-19911. Our modeling studies for L-786134 were in good agreement with the crystal structure data for VK-19911 and showed many of the same inhibitor/enzyme contacts (Figure 2). As shown in Figure 2, most of these residues are conserved in many Ser/Thr kinases. Sequence differences at the primary level are most prominent at residues 106, 107, 108, and 157. It has also been suggested that Met 109 is a key contributor to inhibitor specificity (*26*).

To biochemically test some of these structural and sequence observations, we mutated Met 109 to Ala; Thr 106 to Gln or Met; and Ala 157 to Val. We first measured the steady-state rate constants (Table 1) to assess whether these mutations had any affect on protein substrate binding and/or enzyme activity. All mutants had $K_m$ for GST-ATF2 within approximately 2-fold of wild-type p38, suggesting that the mutations had no effect on protein substrate binding. Since GST-ATF2 and ATP have been shown to be interacting sites in p38 (*24*) and there was no change in the $K_m$ for GST-ATF2 in the mutants, it is likely that all four mutants behave similarly to wild-type p38 with respect to substrate interactions. The $K_m$ for ATP was unchanged compared to wild-type p38 for A157V, M109A, and T106M, indicating that insertion of these residues had no effect on the binding of ATP. The $K_m$(ATP) for T106M = 15 ± 3.4 $\mu$M is in close agreement with $K_m$(ATP) for cAPK = 12.9 ± 0.8 $\mu$M (*43*), a Ser/Thr kinase with Met at the equivalent residue (Figure 2). The $K_m$(ATP) for JNK2, another enzyme with Met at the equivalent residue (Figure 2) was reported to be 2.2 $\mu$M (*44*). The ATP $K_m$ values for p38$\gamma$ and p38$\delta$ have not been reported. In contrast, T106Q had $K_m$ for ATP 17-fold higher than wild-type p38, indicating that ATP exhibits weaker binding to p38 when the larger, more hydrophilic glutamine residue is present at position 106. The ATP $K_m$ for T106Q p38 is in close agreement to the $K_m$ found in ERK2; $K_m$ = 350 ± 60 $\mu$M when Erktide is used as substrate and 190 ± 97 $\mu$M when myelin basic protein (MBP) is used as substrate (*45*). Thus, mutating p38 at position 106 to the equivalent residue in ERK2 made p38 more like ERK2 in ATP binding properties.

The turnover number, $k_{cat}$, was 2−4-fold faster in the mutants A157V, M109A, and T106M, suggesting only a slight change in the properties of the E·S and E·P complexes. The mutant T106Q had $k_{cat}$ 9-fold greater than wild-type p38 (Table 1). Since the rate-determining step for p38 catalysis is not known, it is difficult to speculate as to the cause of the increase in $k_{cat}$. Adams and Taylor (*46*) have shown that ADP-release is rate-limiting for cAPK when an eight amino acid peptide, Kemptide, is the substrate, but when a 20 amino acid peptide is the substrate, phophopeptide-release controls $k_{cat}$ (*47*). Thus, many factors, including the type of substrate, may influence $k_{cat}$.

The bimolecular rate constant, $k_{cat}/K_m$(ATP), was within 2−3-fold of wild-type p38 for the mutants A157V, M109A, and T106Q, indicating that the overall catalytic efficiency for each of these mutants was essentially unchanged. This suggests no gross structural changes in the enzyme occurred as a result of mutagenesis. In the case of T106Q p38, the increase in $k_{cat}$ was offset by an increase in $K_m$ for ATP, leaving the net effect on $k_{cat}/K_m$ relatively unchanged (Table 1). The only mutant that showed a moderate change in $k_{cat}/K_m$(ATP) was T106M (Table 1). One possible explanation for the approximate 7-fold increase in $k_{cat}/K_m$(ATP) is increased interconversion of substrate to product when Met is at position 106. Alternatively, the increase in $k_{cat}/K_m$(ATP) could be a result of increased rate of substrate binding and/or product release. Finally, it should be noted that the 7-fold increase in $k_{cat}/K_m$(ATP) for T106M is different from that seen by Wilson et al. (*28*) who reported no overall change in activity for this mutant. One potential reason for the difference may be due to the different substrates used in the two studies.

The most profound, and easily interpretable effect of mutagenesis was on inhibitor binding (Table 2). Mutation of Thr 106 to Met or Gln (Table 2) resulted in an enzyme that was fully active, yet insensitive to all five inhibitors. This insensitivity is consistent with these inhibitors being much less potent versus ERK2, the JNKs, and cAPK. For example, the diarylimidazoles are >1000-fold more potent and the pyrroles are >350-fold more potent versus p38α than they are versus the JNKs, ERK, or cAPK (O'Keefe et al., unpublished material). The fact that these compounds do inhibit JNK or ERK activity suggest that other residues besides methionine or glutamine may contribute to inhibitor binding in these enzymes. For example, Figure 2 highlights residues such as 107 and 108 that differ from p38α and may be additional contributors to inhibitor binding for the JNKs or ERK.

The most likely explanation for the lack of inhibition in the mutants is that the larger side chains of Met and Gln residues block a key inhibitor binding domain for the *p*-fluorophenyl or *m*-trifluoromethylphenyl rings of the inhibitors. This explanation is borne out in our modeling studies (Figure 4) and is consistent with what was seen in X-ray crystal structures for complexed SB203580 (*27*) and VK-19911 (*28*), which show the *p*-fluorophenyl ring of those two compounds binding in a space not utilized by ATP, yet proximal to the side chain of Thr 106. Moreover, the lack of inhibition for all our compounds in the T106M mutant is consistent with that seen by Wilson et al. (*28*) for the same mutant utilizing VK-19911, a structurally similar compound to those presented in Figure 3.

A second interesting effect on inhibitor binding was seen with the M109A mutant (Table 2). A possible structural explanation for the trends seen in our study is seen in the comparison of the conformation of the Met 109 side chain and the relative positions of the inhibitors in the ATP-binding pocket. L-786134 and L-167307 share a number of contacts between the protein and the moieties at the four and five positions of the scaffold ring. However, L-786134 has an additional hydrogen bond to an imidazole nitrogen and a salt bridge to the piperidinyl nitrogen. These additional contacts draw the inhibitor more deeply into the ATP-binding pocket than L-167307, which lacks these contacts. The position of the pyridinyl ring of L-786134 allows it to better pack with the extended conformation of the side chain of Met 109. An approximately 6-fold loss in affinity of L-786134 resulted upon mutation of Met 109 to Ala, providing evidence for this interaction (Table 2). In contrast, the position of the pyrrole-based inhibitors is too close to the Met 109 side chain in the extended conformation to allow favorable contacts. On the basis of the models, we predicted that, if the Met 109 side chain was held in the extended conformation, an increase in the affinity of the imidazole-based inhibitors and a decrease in the affinity of the pyrrole based inhibitors would be observed.

To address this hypothesis L-786134 was modeled in the ATP-binding site of the p38 mutant A157V (data not shown). The protein−inhibitor contacts described above were preserved and the only change observed was a small displacement of the side chain of Met 109, placing the side chain slightly closer to the pyridyl ring of the inhibitor. An overlay

of the apo structure onto this model suggested that if the Met 109 side chain were in the apo conformation, it would form a close (2.0 Å) contact with the Val 157 side chain. In the valine mutant, the Met 109 side chain is likely to adopt the more extended conformation and would be held in this position by the valine side chain. Holding the Met 109 side chain in the more extended conformation promoted better packing around the pyridyl ring in the imidazole-based inhibitors. On the basis of this model and the L-167307 model, we expected the imidazole-based inhibitors to have a higher affinity for the A157V mutant while the pyrrole-based inhibitors would have a lower affinity. The modeling was consistent with the trends observed in this study (Table 2).

Taken together, our results demonstrated that Thr 106 was a major determinant for p38 inhibitor specificity; groups such as *p*-fluorophenyl and *m*-trifluoromethylphenyl substituents on either imidazole or pyrrole scaffolds can occupy a space near Thr 106; and the side chain of Met 109 increased the binding affinity of imidazole based inhibitors preferentially to pyrrole based inhibitors.

## ACKNOWLEDGMENT

We are grateful to Drs. Jim Doherty, Alice Marcy, and Jed Thompson for critical review of the manuscript. We also thank Dr. Alice Marcy for the pET FLAG vector, Song Zheng for FLAG peptide, and Tracey Klatt for mass spectrometry.

## REFERENCES

1. Hunter, T. (1991) *Methods Enzymol. 200*, 3−37.
2. Pearson, R. B., and Kemp, B. E. (1991) *Methods Enzymol. 200*, 62−81.
3. Bruton, V. G., and Workman, P. (1993) *Cancer Chem. Pharmacol. 32*, 1−19.
4. Powis, G. (1994) *Pharmacol. Ther. 62*, 57−95.
5. Elder, J. J., Fisher, G. L., Lindquist, P. B., Bennet, G. L., Pittelkow, M. R., Coffey, R. J., Ellingsworth, L., Denryneck, R., and Voorhees, J. J. (1989) *Science 243*, 811−814.
6. Ross, R. (1993) *Nautre 362*, 801−809.
7. Lee, J. C., Badger, A. M., Griswold, D. E., Dunnington, D., Truneh, A., Votta, B., White, J. R., Young, P. R., and Bender, P. E. (1993) *Ann. N. Y. Acad. Sci. 696*, 149−170.
8. Badger, A. M., Bradbeer, J. N., Votta, B., Lee, J. C., Adams, J. L., and Griswold D. E. (1996) *J. Pharm., Exp. Ther. 279*, 1453−1461.
9. Fry, D. W., Kraker, A. J., McMichael, A., Ambroso, L. A., Nelson, J. M., Leopold, W. R., Conners, R. W., and Briggs, A. J. (1994) *Science 265*, 1093−1095.
10. Levitzki, A., and Gavit, A. (1995) *Science 267*, 1782−1788.
11. Fry, D. W., and Briggs, A. J. (1995) *Curr. Opin. Biotechnol. 6*, 662−667.
12. Lee, J. C., Laydon, J. T., McDonnell, P. C., Gallagher, T. F., Kumar, S., Green, D., McNulty, D., Blumnethal, M. J., Heys, J. R., Landvatter, S. W., Strickler, J. E., McLaughlin, M. M., Siemens, I. R., Fisher, S. M., Livi, G. P., White, J. R., Adams, J. L., and Young, P. R. (1994) *Nature 372*, 739−746.
13. Reddy, M. P., Webb, E. F., Cassatt, D., Maley, D., Lee, J. C., Griswold, D. E., and Truneh, A. (1994) *J. Immunol. Pharmacol. 16*, 795−803.
14. Cuenda, A., Rouse, J., Doza, Y. N., Meier, R., Cohen, P., Gallagher, T. F., Young, P. R., and Lee, J. C. (1995) *FEBS Lett. 364*, 229−233.
15. Gallagher, T. F., Seibel, G. L., Kassis, S., Laydon, J. T., Blumnethal, M. J., Lee, J. C., Lee, D., Boehm, J. C., Thompson-Fier, S. M., Abt, J. W., Soreson, M. E., Smietana, J. M., Hall, R. F., Garigipati, R. S., Bender, P. E., Erhard, K. F., Krog, A. J., Hofmann, G. A., Sheldrake, P. L., McDonnell, P. C., Kumar, K. F., Young, P. R., and Adams, J. A. (1997) *Bioorg. Med. Chem. 5*, 49−64.
16. Han, J., Lee, J.-D., Tobias, P. S., and Ulevitch, R. J. (1993) *J. Biol. Chem. 268*, 25009−25014.
17. Han, J., Lee, J.-D., Bibbs, L., and Ulevitch, R. J. (1994) *Science 265*, 808−811.
18. Raingeaud, J., Gupta, S., Rogers, J. S., Dickens, M., Han, J., Ulevitch, R. J., and Davis, R. J. (1995) *J. Biol. Chem. 270*, 7420−7426.
19. Han, J., Lee, J.-D., Jiang, Y., Li, Z., Feng, L., and Ulevitch, R. J. (1996) *J. Biol. Chem. 271*, 2886−2891.
20. Raingeaud, J., Whitmarsh, A. J., Barrett, T., Derijard, B., and Davis, R. J. (1996) *Mol. Cell. Biol. 16*, 1247−1255.
21. Han, J., Wang, X., Jiang Y., Ulevitch, R. J., and Lin, S. (1997) *FEBS Lett. 403*, 19−22.
22. Rouse, J., Cohen, P., Trigon, S., Morange, M., Alonso-Llamazares, A., Zamanillo, D., Hunt, T., and Nebreda, A. (1994) *Cell 78*, 1027−1037.
23. McLaughlin, M. M., Kumar, S., McDonnell, P. C., Van Horn, S., Lee, J. C., Livi, G. P., and Young, P. R. (1996) *J. Biol. Chem. 271*, 8488−8492.
24. LoGrasso, P. V., Frantz, B., Rolando, A. M., O'Keefe, S. J., Hermes, J. D., and O'Neill, E. A. (1997) *Biochemistry 36*, 10422−10427.
25. Wilson, K. P., Fitzgibbon, M. J., Caron, P. R., Griffith, J. P., Chen, W., McCaffrey, P. G., Chambers, S. P., and Su, S.-S., M. (1996) *J. Biol. Chem. 271*, 27696−27700.
26. Wang, Z., Harkins, P. C., Ulevitch, R. J., Han, J., Cobb, M. H., and Goldsmith, E. J. (1997) *Proc. Natl. Acad. Sci. 94*, 2327−2332.
27. Tong, L., Pav, S., White, D. M., Rogers, S., Crane, K. M., Cywin, C. L., Brown, M. L., and Pargellis, C. A. (1997) *Nat. Struct. Biol. 4*, 311−316.
28. Wilson, K. P., McCaffrey, P. G., Hsiao, K., Pazhanisamy, S., Galullo, V., Bemis, G. W., Fitzgibbon, M. J., Caron, P. R., Murcko, M. A., and Su, S.-S., M. (1997) *Chem. Biol. 4*, 423−431.
29. Yamaguchi, H., and Hendrickson, W. A. (1996) *Nature 384*, 484−489.
30. Engh, R. A., Girod, A., Kinzel, V., Huber, R., and Bossemeyer, D. (1996) *J. Biol. Chem. 271*, 26157−26164.
31. de Azevedo, W. F., Jr., Mueller-Dieckmann, H.-J., Schulze-Gahmen, U., Worland, P. J., Sausville, E., and Kim, S.-H. (1996) *Proc. Natl. Acad. Sci. 93*, 2735−2740.
32. Xu, R.-H., Carmel, G., Kuret, J., and Cheng, X. (1996) *Proc. Natl. Acad. Sci. 93*, 6308−6313.
33. Traxler, P. M., Furet, P., Mett, H., Buchdunger, E., Meyer, T., and Lydon, N. (1996) *J. Med. Chem. 39*, 2285−2292.
34. Young, P. R., McLaughlin, M. M., Kumar, S., Kassis, S., Doyle, M. L., McNulty, D., Gallagher, T. F., Fisher, S., McDonnell, P. C., Carr, S. A., Huddleston, M. J., Seibel, G., Porter, T. G., Livi, G. P., Adams, J. L., and Lee, J. C. (1997) *J. Biol. Chem. 272*, 12116−12121.
35. Kovalenko, M., Ronnstrand, L., Heldin, C.-H., Loubtchenkov, M., Gazit, A., Levitzki, A., and Bohmer, F. D. (1997) *Biochemistry 36*, 6260−6269.
36. Wells, J. A., Vasser, M., and Powers, D. B. (1985) *Gene 34*, 315−323.
37. Steller, H., and Pirrotta, V. (1985) *EMBO J. 4*, 167−171.
38. Bunch, T. A., Grinblat, Y., and Goldstein, L. S. B. (1988) *Nucleic Acid Res. 16*, 1043−1061.
39. Leatherbarrow, R. J. (1992) *GraFit*, version 3.0, Erithacus Software Ltd. Staines, United Kingdom.
40. de Laszlo, S. E., Agarwal, L., Chang, L., Chin, J., Croft, G., Forsyth, A., Fletcher, D., Frantz, B., Hacker, C., Hanlon, W., Harper, C., Kostura, M., Li, B., Luell, S., MacCoss, M., Mantlo, N., O'Neill, E., Orevillo, C., Pang, M., Parsons, J., Rolando, A., Sahly, Y., Sidler, K., Widmer, W. R., Visco, D., and O'Keefe, S. (1998) *Pathogenesis of Rheumatoid Arthritis: Implications for Future Therapy. Keystone Symposia*, Tamaron, CO, January 23−29, 1998 (Abstr. 213).

41. Hanke, J. H., Gardner, J. P., Dow, R. L., Changelian, P. S., Brissette, W. H., Weringer, E. J., Pollok, B. A., and Connelly, P. A. (1996) *J. Biol. Chem. 271*, 695−701.
42. Rewcastle, G. W., Palmer, B. D., Thompson, A. M., Bridges, A. J., Cody, D. R., Zhou, H., Fry, D. W., McMichael, A., and Denny, W. A. (1996) *J. Med. Chem. 39*, 1823−1835.
43. Cook, P. F., Neville, M. E., Jr., Vrana, K. E., Hartl, T., and Roskoski, R., Jr. (1982) *Biochemistry 21*, 5794−5799.
44. Anderson, D. (1997) The National Health Care Congress: Cell Signaling, San Diego, CA, July 9−11, 1997.
45. Robinson, M. J., Harkins, P. C., Zhang, J., Baer, R., Haycock, J. W., Cobb, M. H., and Goldsmith, E. J. (1996) *Biochemistry 35*, 5641−5646.
46. Adams, J. A., and Taylor, S. S. (1992) *Biochemistry 31*, 8516−8522.
47. Madhusdan, E. A., Trafny, N.-H, X., Adams, J. A., Ten Eyck, L. F., Taylor, S. S., and Sowadski, J. M. (1994) *Protein Sci. 3*, 176−187.

BI981591X